Journal of Geoscience and Environment Protection, 2024, 12, 138-146
https://www.scirp.org/journal/gep
ISSN Online: 2327-4344
ISSN Print: 2327-4336

Correction of Error Due to Vessel Movement in Underwater Topographic Data Measurement

Satoshi Iwakami[1], Masahiko Tamega[1], Masahide Sanada[1], Michiaki Mohri[1], Yoshitaka Iwakami[1], Naoki Okamoto[1], Eishi Mitsui[1], Hidetaka Chikamori[2], Ryosuke Akoh[3], Shuji Jimbo[4*], Masaji Watanabe[4#]

[1]Earth Rise Company, Inc., Okayama, Japan
[2]Architecture, Civil Engineering and Environmental Management Program, Faculty of Engineering, Okayama University, Okayama, Japan
[3]Mechanical Systems and Urban Innovation Sciences, Graduate School of Environmental, Life, Natural Science and Technology, Okayama University, Okayama, Japan
[4]Okayama University, Okayama, Japan
Email: watan-m@okayama-u.ac.jp

How to cite this paper: Iwakami, S., Tamega, M., Sanada, M., Mohri, M., Iwakami, Y., Okamoto, N., Mitsui, E., Chikamori, H., Akoh, R., Jimbo, S., & Watanabe, M. (2024). Correction of Error Due to Vessel Movement in Underwater Topographic Data Measurement. *Journal of Geoscience and Environment Protection, 12,* 138-146.
https://doi.org/10.4236/gep.2024.124010

Received: April 3, 2024
Accepted: April 27, 2024
Published: April 30, 2024

Abstract

In underwater topographic measurement implementing the positioning by a GPS receiver and/or a GNSS receiver and the depth measurement by an echo sounder, an antenna connected to a GPS receiver or a GNSS receiver and a transreceiver of the echosounder are fixed to a vessel. On the other hand, a vessel is subject to movements such as longitudinal swayings (roll), sideways swayings (pitch), and bow swayings (yaw), which result in errors of output data. This study shows techniques to compensate for those errors.

Keywords

Underwater Topography, Positioning, Depth measurement, Vessel Movement, Error Compensation

1. Introduction

Disastrous heavy rain events in recent years indicate a manifestation of the global warming. One speculation is that those events may increase in frequency and scale as the climate change progresses, and the maintenance of rivers, reservoirs, and coastal areas as well as measurement and analysis for the topography of water areas are necessary. This study focuses on a measurement aspect of the topography of water areas.

*Guest Researcher.
#Emeritus Professor, Specially Appointed Professor (Research).

In our measurement of underwater topography, the positioning by a GPS receiver and/or a GNSS receiver and the depth measurement by an echo sounder are implemented (Iwakami et al., 2019, 2020, 2021a, 2021b, 2023a, 2023b, 2023c). A GPS receiver or a GNSS receiver outputs positions of the antenna connected to it. An echo sounder transmits and receives sound waves emanated from the tip of its transreceiver (transmitter and receiver) and outputs its distance from the bottom. In our measurement, a GPS antenna and/or a GNSS antenna, and a transreceiver are fixed to a boat. On the other hand, a boat is subject to movements such as longitudinal swayings (roll), sideways swayings (pitch), and bow swayings (yaw), which lead to errors in output data. The following sections discuss errors due to the movements of the boat, and how to compensate them.

Basically, an echo sounder outputs the shortest distance among ones that sound waves reflected from a bottom generate. The intensity of sound waves reduces by half on the surface of a cone with the apex at the transreceiver. The angle made by half lines intersected by the cone and a plane containing a center line of the cone is called the directional angle or the angle of beam spread (Based on information provided by Senbondenki Co., Ltd.). The following sections develop analyses based on assumption that an echo sounder outputs the shortest distance among ones corresponding to sound waves restricted to the region enclosed by the cone.

2. Basic Properties of Sound Waves

2.1. Equations of Cone and Ellipse

Consider a cone and a plane that does not pass through the apex of the cone. A curve obtained by intersecting such a cone and a plane is called a conic section. In general, a conic section is either a parabola, an ellipse, or a hyperbola (Apostol, 1967). This section focuses on an ellipse as a conic section in an *xy* plane.

Let σ denote the directional angle (**Figure 1**). Note that condition $0 < \sigma < \pi$ holds. Denote by $\boldsymbol{i}$, $\boldsymbol{j}$, and $\boldsymbol{k}$ the unit coordinate vectors in a three-dimensional space pointing the positive directions of *x*, *y*, and *z* axes, respectively. Denote by *P* the point on the positive *z* axis, whose distance from the origin equals *r*. That is, *P* (0, 0, *r*). Let $\boldsymbol{v}$ denote the unit vector $\alpha\boldsymbol{i} + \beta\boldsymbol{j} + \gamma\boldsymbol{k}$ that satisfies the conditions $\alpha^2 + \beta^2 + \gamma^2 = 1$ and $-1 \le \gamma < 0$. Consider the half line $\boldsymbol{K}$ with its end at the point *P* in the direction of the vector **v**.

Suppose that the end point of a half line $\boldsymbol{M}$ is *P*, and that the angle made by the half line $\boldsymbol{M}$ and the half line $\boldsymbol{K}$ is σ/2. Let $\boldsymbol{C}$ denote the cone generated by rotating the half line $\boldsymbol{M}$ about the half line $\boldsymbol{K}$. Let ω denote the angle made by the vector $\boldsymbol{v}$ and the vector $-\boldsymbol{k}$, Note that ω is given by the expressions

$$\omega = \tan^{-1}\frac{\sqrt{\alpha^2+\beta^2}}{|\gamma|},\ \omega = \tan^{-1}\frac{\sqrt{1-\gamma^2}}{|\gamma|},\ \text{or}\ \omega = \cos^{-1}|\gamma|.$$

Suppose that $Q(x, y, z)$ is a point on the cone $\boldsymbol{C}$. A point *R* on the half line $\boldsymbol{K}$ is expressible in the form $R(\tau\alpha, \tau\beta, r + \tau\gamma)$, where the parameter τ denotes the distance between *P* and *R*. In particular, the half line $\boldsymbol{K}$ and the line passing

through Q meet at the point R perpendicularly for $\tau = \alpha x + \beta y + \gamma(z-r)$. Let l denote the distance between the point Q and the point R. Then the equation

$$l^2 = (x-\tau\alpha)^2 + (y-\tau\beta)^2 + (z-r-\tau\gamma)^2$$

holds (**Figure 2**). The condition

$$l^2 = \left(\tan\frac{\sigma}{2}\right)^2 \tau^2$$

leads to the equation of the cone $\boldsymbol{C}$

$$\begin{aligned}&(1-\alpha^2)x^2 + (1-\beta^2)y^2 + (1-\gamma^2)(z-r)^2 - 2\alpha\beta xy - 2\alpha\gamma x(z-r)\\ &-2\beta\gamma y(z-r) - \left[\tan\left(\frac{\sigma}{2}\right)\right]^2 [\alpha x + \beta y + \gamma(z-r)]^2 = 0.\end{aligned} \tag{1}$$

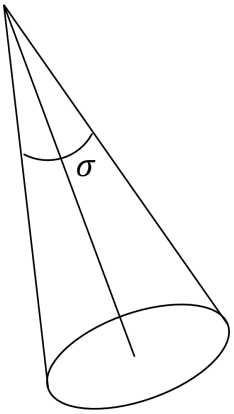

Figure 1. Cone generated by valid sound waves and the directional angle σ.

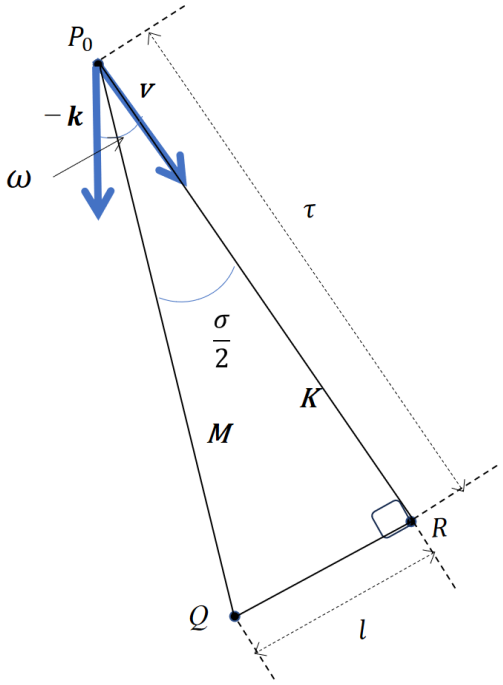

Figure 2. Half line generating the cone and the half line ***K***.

The intersection of the cone C and the xy plane is an ellipse, which we denote by E. Substitution $z=0$ into the Equation (1) yields the equation of the ellipse E

$$\begin{aligned}&\left(1-\alpha^2\right)x^2+\left(1-\beta^2\right)y^2+\left(1-\gamma^2\right)r^2-2\alpha\beta xy+2\alpha\gamma rx+2\beta\gamma ry\\&-\left[\tan\left(\frac{\sigma}{2}\right)\right]^2\left(\alpha x+\beta y-\gamma r\right)^2=0.\end{aligned}\tag{2}$$

2.2. Extremum Distance from Apex to Horizontal Plane

Define the function $g(x,y)$ by the expression

$$\begin{aligned}g(x,y)=&\left\{\left[\cos\left(\frac{\sigma}{2}\right)\right]^2-\alpha^2\right\}x^2+\left\{\left[\cos\left(\frac{\sigma}{2}\right)\right]^2-\beta^2\right\}y^2-2\alpha\beta xy\\&+2\alpha\gamma rx+2\beta\gamma ry+\left\{\left[\cos\left(\frac{\sigma}{2}\right)\right]^2-\gamma^2\right\}r^2\end{aligned}$$

Equation (2) converts to the equation

$$g(x,y)=0.\tag{3}$$

Substitution $x=\alpha\rho/\sqrt{1-\gamma^2}$, $y=\beta\rho/\sqrt{1-\gamma^2}$ into the function $g(x,y)$ yields the function $h(\rho)$ defined by the expression

$$\begin{aligned}h(\rho)&=g\left(\frac{\alpha\rho}{\sqrt{1-\gamma^2}},\frac{\beta\rho}{\sqrt{1-\gamma^2}}\right)\\&=\left\{\gamma^2-\left[\sin\left(\frac{\sigma}{2}\right)\right]^2\right\}\rho^2+2\gamma\sqrt{1-\gamma^2}r\rho+\left\{\left[\cos\frac{\sigma}{2}\right]^2-\gamma^2\right\}r^2.\end{aligned}$$

Define values ρ_- and ρ_+ of the parameter ρ by the expressions

$$\begin{aligned}\rho_-&=r\tan\left(\omega-\frac{\sigma}{2}\right)=r\frac{|\gamma|\sqrt{1-\gamma^2}-\cos\frac{\sigma}{2}\sin\frac{\sigma}{2}}{\gamma^2-\left(\sin\frac{\sigma}{2}\right)^2},\\\rho_+&=r\tan\left(\omega+\frac{\sigma}{2}\right)=r\frac{|\gamma|\sqrt{1-\gamma^2}+\cos\frac{\sigma}{2}\sin\frac{\sigma}{2}}{\gamma^2-\left(\sin\frac{\sigma}{2}\right)^2}.\end{aligned}\tag{4}$$

Then ρ_- and ρ_+ are solutions of the equation $h(\rho)=0$ (**Figure 3**). Define values x_-, y_-, x_+, and y_+

$$\begin{aligned}x_-&=\frac{\alpha\rho_-}{\sqrt{1-\gamma^2}}=\frac{\alpha r}{\sqrt{1-\gamma^2}}\tan\left(\omega-\frac{\sigma}{2}\right),\\y_-&=\frac{\beta\rho_-}{\sqrt{1-\gamma^2}}=\frac{\beta r}{\sqrt{1-\gamma^2}}\tan\left(\omega-\frac{\sigma}{2}\right),\\x_+&=\frac{\alpha\rho_+}{\sqrt{1-\gamma^2}}=\frac{\alpha r}{\sqrt{1-\gamma^2}}\tan\left(\omega+\frac{\sigma}{2}\right),\\y_+&=\frac{\beta\rho_+}{\sqrt{1-\gamma^2}}=\frac{\beta r}{\sqrt{1-\gamma^2}}\tan\left(\omega+\frac{\sigma}{2}\right).\end{aligned}\tag{5}$$

The pairs (x_-, y_-) and (x_+, y_+) are solutions of the equation (3)

$$g(x_-, y_-) = 0, \quad g(x_+, y_+) = 0. \tag{6}$$

Denote by P_- and P_+ the points whose x coordinates and y coordinates are x_- and y_-, and x_+ and y_+, respectively. The z coordinates of P_- and P_+ are zero (**Figure 3**). In what follows, the method of Lagrange's multipliers (Apostol, 1969) leads to the conclusion that the minimum and the maximum of the distances between the peak of the cone P and points in the region of the xy plane enclosed by the ellipse $\boldsymbol{E}$ are attained at the points P_- and P_+, respectively.

Define a function f by the expression $f(x, y) = x^2 + y^2$. Then, the partial derivatives of f are given by the expressions

$$\frac{\partial f}{\partial x} = 2x, \quad \frac{\partial f}{\partial y} = 2y.$$

On the other hand, the partial derivatives of g are given by the expressions

$$\frac{\partial g}{\partial x} = 2\left\{\left[\left(\cos\frac{\sigma}{2}\right)^2 - \alpha^2\right]x - \alpha\beta y + \alpha\gamma r\right\},$$

$$\frac{\partial g}{\partial y} = 2\left\{\left[\left(\cos\frac{\sigma}{2}\right)^2 - \beta^2\right]y - \alpha\beta x + \beta\gamma r\right\}.$$

Define a function $u(\rho)$ by the expression

$$u(\rho) = \rho\left(\cos\frac{\sigma}{2}\right)^2 - \rho + \gamma r\sqrt{1-\gamma^2}.$$

For $x = \alpha\rho/\sqrt{1-\gamma^2}$, $y = \beta\rho/\sqrt{1-\gamma^2}$ $(\rho > 0)$,

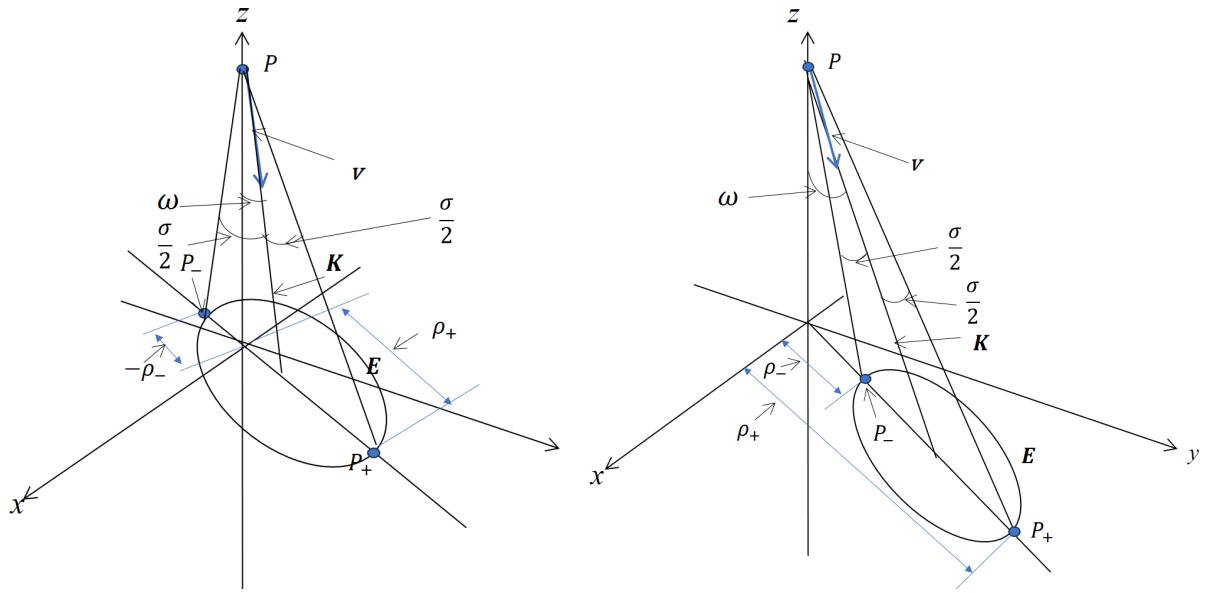

Figure 3. (a) $\sigma/2 > \omega$; (b) $\sigma/2 < \omega$.

$$\left[\left(\cos\frac{\sigma}{2}\right)^2-\alpha^2\right]x-\alpha\beta y+\alpha\gamma r=\frac{\alpha}{\sqrt{1-\gamma^2}}u(\rho),$$

$$\left[\left(\cos\frac{\sigma}{2}\right)^2-\beta^2\right]y-\alpha\beta x+\beta\gamma r=\frac{\beta}{\sqrt{1-\gamma^2}}u(\rho),$$

and

$$\frac{\frac{\partial g}{\partial x}}{\frac{\partial f}{\partial x}}=\frac{\frac{\alpha}{\sqrt{1-\gamma^2}}u(\rho)}{\frac{\alpha\rho}{\sqrt{1-\gamma^2}}}=\frac{u(\rho)}{\rho},\quad \frac{\frac{\partial g}{\partial y}}{\frac{\partial f}{\partial y}}=\frac{\frac{\beta}{\sqrt{1-\gamma^2}}u(\rho)}{\frac{\beta\rho}{\sqrt{1-\gamma^2}}}=\frac{u(\rho)}{\rho}.$$

For any point on the half line in the *xy* plane, $x=\alpha\rho/\sqrt{1-\gamma^2}$, $y=\beta\rho/\sqrt{1-\gamma^2}$ ($\rho>0$), the gradients of the functions *f* and *g* are parallel, that is, the equation

$$\nabla g=\frac{u(\rho)}{\rho}\nabla f \tag{7}$$

holds, where ∇f and ∇g denote the gradients of *f* and *g*, respectively. In particular, the equation (7) holds for the points P_- and P_+.

Suppose that $\sigma/2<\omega$, Equations (4) and (5) show that the circles in the *xy* plane with the centers at the origin and the radii ρ_- and ρ_+ are tangent to the ellipse $\boldsymbol{E}$ at the points P_- and P_+ (**Figure 3(b)**), respectively. This means that the circle centered at the origin with the radius ρ_- contains no point in the region enclosed by the ellipse *E* except P_- and that the circle centered at the origin with the radius ρ_+ contains *E*. It follows that the pair of values (x_-, y_-) minimizes the value of the function $f(x,y)=x^2+y^2$ and hence the value of the expression $x^2+y^2+r^2$. The foregoing discussion leads to the conclusion that the pair of values (x_-, y_-) minimize the distance $\sqrt{x^2+y^2+r^2}$ between the apex *P* of the cone $\boldsymbol{C}$ and the points $(x, y, 0)$ in the region enclosed by the ellipse $\boldsymbol{E}$ intersected by the cone $\boldsymbol{C}$ and the *xy* plane. For $\sigma/2\geq\omega$, ellipse $\boldsymbol{E}$ contains the origin (**Figure 3(a)**). In this case distance between the point *P* and the origin is the minimum among distances between the point *P* and points in the *xy* plane, including points in the region enclosed by $\boldsymbol{E}$.

3. Implementation of Error Compensation Techniques in Measurement Data Analysis

3.1. Positioning Data and Depth Data Error Compensation

In our measurement of underwater topographic data, a GPS antenna and/or a GNSS antenna is attached to the upper end of a prop and a transreceiver of an echo sounder is attached to the lower end of the prop in the water. Let *L* denote the distance between the center of a GPS antenna and the transreceiver of an echo sounder. Let $\boldsymbol{v}$ denote the unit vector $\alpha\boldsymbol{i}+\beta\boldsymbol{j}+\gamma\boldsymbol{k}$ that satisfies the conditions $\alpha^2+\beta^2+\gamma^2=1$ and $-1\leq\gamma<0$. Suppose that $\boldsymbol{v}$ points in the direction of the center line of the cone of intensity reduction by half, which is an extension

of the prop.

Suppose that $P_0(x_0, y_0, z_0)$ denotes the point at which the center of the antenna is located, and that $P_1(x_1, y_1, z_1)$ denotes the point at which the transreceiver is located. Note that P_1 is given by the expression $P_1 = P_0 + L\boldsymbol{v}$, that is,

$$x_1 = x_0 + L\alpha,\ \ y_1 = y_0 + L\beta,\ \ z_1 = z_0 + L\gamma.$$

Let $P_2(x_2, y_2, z_2)$ denote the point at which a sound wave from the transreceiver was reflected for the echo sounder to generate an output result. Let d denote an echo sounder output. As was shown in the previous section, the location of P_2 depends on values of the parameters σ and ω. Suppose that $\sigma/2 \geq \omega$ (**Figure 4(a)**). In this case,

$$x_2 = x_1 = x_0 + L\alpha,\ \ y_2 = y_1 = y_0 + L\beta,\ \ z_2 = z_1 - d = z_0 + L\gamma - d. \tag{8}$$

Suppose that $\sigma/2 < \omega$ (**Figure 4(b)**). For $r = d\cos(\omega - \sigma/2)$, expressions (5) for x_- and y_- become

$$x_- = \frac{\alpha d}{\sqrt{1-\gamma^2}}\sin\left(\omega - \frac{\sigma}{2}\right),$$

$$y_- = \frac{\beta d}{\sqrt{1-\gamma^2}}\sin\left(\omega - \frac{\sigma}{2}\right),$$

which lead to the expressions of x_2, y_2, and z_2;

$$x_2 = x_1 + \frac{\alpha d}{\sqrt{1-\gamma^2}}\sin\left(\omega - \frac{\sigma}{2}\right) = x_0 + L\alpha + \frac{\alpha d}{\sqrt{1-\gamma^2}}\sin\left(\omega - \frac{\sigma}{2}\right), \tag{9}$$

$$y_2 = y_1 + \frac{\beta d}{\sqrt{1-\gamma^2}}\sin\left(\omega - \frac{\sigma}{2}\right) = y_0 + L\beta + \frac{\beta d}{\sqrt{1-\gamma^2}}\sin\left(\omega - \frac{\sigma}{2}\right), \tag{10}$$

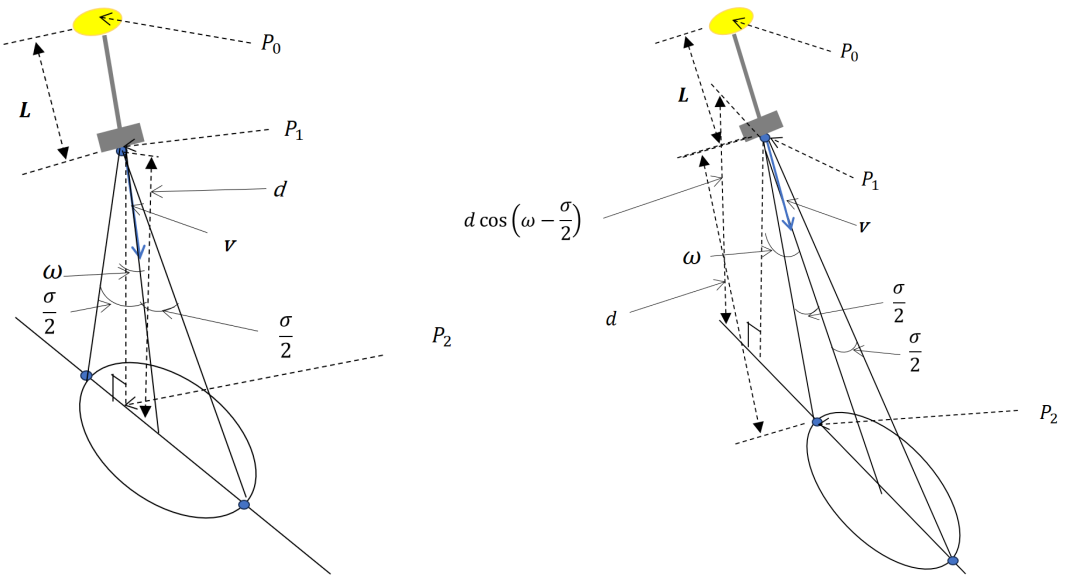

Figure 4. (a) $\sigma/2 > \omega$; (b) $\sigma/2 < \omega$.

$$z_2 = z_1 - d\cos\left(\omega - \frac{\sigma}{2}\right) = z_0 + L\gamma - d\cos\left(\omega - \frac{\sigma}{2}\right).$$

3.2. Amount of Error in Measurement Data

Suppose that $P_1'(x_1', y_1', z_1')$ denotes the point at which the transreceiver is located without error compensation, and that $P_2'(x_2', y_2', z_2')$ denote the point at which a sound wave from the transreceiver was reflected for the echo sounder to generate an output result without error compensation. Then the coronates of $P_1'(x_1', y_1', z_1')$ and $P_2'(x_2', y_2', z_2')$ are given by the expressions

$$x_1' = x_0,\ \ y_1' = y_0,\ \ z_1' = z_0 - L,$$

and

$$x_2' = x_1' = x_0,\ \ y_2' = y_1' = y_0,\ \ z_2' = z_1' - d = z_0 - L - d. \tag{11}$$

For $\sigma/2 \geq \omega$, expressions (8) and (11) lead to the square of the distance between P_2 and P_2'

$$\begin{aligned}&(x_2 - x_2')^2 + (y_2 - y_2')^2 + (z_2 - z_2')^2 = (L\alpha)^2 + (L\beta)^2 + (L\gamma + L)^2\\ &= L^2\left[\alpha^2 + \beta^2 + (\gamma + 1)^2\right] = 2L^2(1 + \gamma).\end{aligned}$$

For $\sigma/2 \geq \omega$, expressions (9), (10), and (11) lead to the error

$$\begin{aligned}&(x_2 - x_2')^2 + (y_2 - y_2')^2 + (z_2 - z_2')^2\\ &= (\alpha^2 + \beta^2)\left[L + \frac{d}{\sqrt{1-\gamma^2}}\sin\left(\omega - \frac{\sigma}{2}\right)\right]^2 + \left\{L(1+\gamma) + d\left[1 - \cos\left(\omega - \frac{\sigma}{2}\right)\right]\right\}^2.\end{aligned}$$

4. Discussion

In the topographic measurement of water areas such as rivers, reservoirs, or coastal areas, a small vessel is more flexible than large one. On the other hand, small vessels are more susceptible to wind and waves than large ones. This study established techniques for the correction of errors due to the movement of a vessel in the topographic measurement of water areas.

Our future issues include verification of our techniques for correction of errors due to movements and development of a hardware-software system for reliable measurement. They also include application of our techniques to scheduled measurement to investigate topographic changes, and the comparison between numerical results and measurement results.

Funding

This study was supported by 2020-2021 Research Grant from the Public Interest Incorporated Foundation, Wesco Scientific Promotion Foundation, Public Interest Incorporated Foundation, The Yakumo Foundation for Environmental Science 2022 Research Grant, and General Incorporated Foundation, The Japan Homeland Development Future Research Foundation 2022-2023 Academic Research Grant.

Conflicts of Interest

The authors declare no conflicts of interest regarding the publication of this paper.

References

Apostol, T. M. (1967). *CALCULUS, Volume 1, One-Variable Calculus, with an Introduction to Linear Algebra* (2nd ed.). John Wiley & Sons, Inc.

Apostol, T. M. (1969). *CALCULUS, Volume II, Multi Variable Calculus and Linear Algebra, with Applications to Differential Equations and Probability* (2nd ed.). John Wiley & Sons, Inc.

Iwakami, S. Tamega, M., Sanada, M., Mohri, M., Iwakami, Y, Okamoto, N., Mitsui, E., Chikamori, H., Akoh, R., Jimbo, S., & Watanabe, M. (2023a). Measurement and Computational Study of Underwater Topography. *Journal of Geoscience and Environmental Protection*, *11*, 203-209. https://doi.org/10.4236/gep.2023.114012 https://www.scirp.org/journal/paperinformation.aspx?paperid=124959

Iwakami, S., Tamega, M., Jimbo, S., & Watanabe, M. (2019). Numerical Techniques for Underwater Topographic Measurement with GPS and Echo Sounder. *International Journal of Information System & Technology*, *3*, 81-85. http://ijistech.org/ijistech/index.php/ijistech/article/view/37

Iwakami, S., Tamega, M., Sanada, M., Mohri, M., Iwakami, Y., Jimbo, S., & Watanabe, M (2020). Study of Underwater Topography Change with Measurement and Analysis. *Journal of Physics: Conference Series*, *1641*, 012003. https://doi.org/10.1088/1742-6596/1641/1/012003 https://iopscience.iop.org/article/10.1088/1742-6596/1641/1/012003/pdf

Iwakami, S., Tamega, M., Sanada, M., Mohri, M., Iwakami, Y., Okamoto, N., Jimbo, S., & Watanabe, M. (2021a). Study on Change of Topography in Water Area with Field Measurement. *Journal of Geoscience and Environmental Protection*, *9*, 221-226. https://www.scirp.org/journal/paperinformation.aspx?paperid=109431

Iwakami, S., Tamega, M., Sanada, M., Mohri, M., Iwakami, Y., Okamoto, N., Asou, R., Jimbo, S., & Watanabe, M. (2021b). Mathematical Modeling and Computational Analysis of Underwater Topography with Global Positioning and Echo Sounder Data. *Journal of Applied Mathematics and Physics*, *9*, 1171-1179. https://www.scirp.org/journal/paperinformation.aspx?paperid=109663

Iwakami, S., Tamega, M., Sanada, M., Mohri, M., Iwakami, Y., Okamoto, N., Mitsui, E., Jimbo, S., & Watanabe, M. (2023b). Issues Associated with Construction of Underwater Topography and Analytical Techniques for Measurement Results, Industrial Materials. *Bulletin of the Japan Society for Industrial and Applied Mathematics*, *33*, 32-39. (In Japanese)

Iwakami, S., Tamega, M., Sanada, M., Mohri, M., Iwakami, Y., Okamoto, N., Asou, R., Jimbo, S., & Watanabe, M. (2023c). Numerical Study of Underwater Topography with Measurement Data. *AIP Conference Proceedings*, *2714*, 030014. https://doi.org/10.1063/5.0128371 https://pubs.aip.org/aip/acp/issue/2714/1